Leadership in Sustainable Infrastructure

Leadership en Infrastructures Durables

Vancouver, Canada

May 31 – June 3, 2017/ *Mai 31 – Juin 3, 2017*

EFFECT OF BRACING HEIGHT ON LATERAL TORSIONAL BUCKLING RESISTANCE OF STEEL BEAMS

Pezeshky, Payam[1], Sahraei, Arash[2] and Mohareb, Magdi[3,4]
[1] Graduate research assistant, University of Ottawa, Canada
[2] Graduate research assistant, University of Ottawa, Canada
[3] Professor, University of Ottawa, Canada
[4] MagdiEmile.Mohareb@uottawa.ca

Abstract:

Present beam analysis techniques for determining the elastic lateral torsional buckling resistance for beams enable the modelling of intermediate lateral braces located at section mid-height. In practical design situations however, either top or bottom flange bracing may be provided. Such bracing conditions have received little attention in the literature. The present study investigates the effect of bracing height on the elastic lateral torsional buckling resistance of beams. In each case, three eigen-value buckling solutions are conducted: (1) a shell-based finite element solution, (2) a newly developed beam finite element that captures distortional buckling effects, and (3) a non-distortional Vlasov thin-walled beam buckling element modified to account for top and/or bottom flange bracing. The three models are used to investigate the elastic lateral torsional buckling for cantilevers under tip loads and simply supported beams under point loads. An assessment is then provided on the effect of various bracing scenarios and distortional effects on the predicted critical moments. Comparisons with shell analysis illustrate the versatility of the finite elements developed in comparison to existing standard procedures in quantifying the critical moments for beams with braces offset from the shear center.

Keywords: Finite element analysis, Bracing height effect, Lateral torsional buckling, Distortion

1 INTRODUCTION AND LITERATURE REVIEW

Design provisions in structural steel standards (e.g., CAN/CSA-S16 (2014), ANSI/AISC-360 (2016)) provide guidelines for determining the lateral torsional buckling (LTB) resistance for beams where both ends of the beam are restrained against lateral displacements and twist. Simplified recommendations are provided for cantilevers. In both cases, the underlying formulation is based on the Vlasov thin-walled beam theory (Vlasov 1961) which neglects web distortion. Present design provisions are applicable to cases where intermediate points provide full lateral and torsional restraints. In such cases, the unsupported length is taken as the distance between points of lateral and torsional support. No guidelines are provided in CAN/CSA-S16 (2014) for cases where intermediate points are braced laterally either at the top or at the bottom flanges, but unbraced against twist.

Barsoum and Gallagher (1970) developed a finite element based on the Vlasov thin-walled beam kinematics (Vlasov (1961) to predict the lateral torsional buckling resistance of the beams. Trahair (1993)

provided a comprehensive review of theoretical developments related to lateral torsional buckling of beams under various boundary conditions, loading schemes and bracing scenarios. In the majority of the work, web distortion is considered negligible in line with the postulated Vlasov kinematics. Neville et al. (1984) Investigated the LTB of the cantilever I-beams with discrete lateral/torsional restraints subjected to concentrated and uniformly distributed loads. The numerical solutions were compared to experimental results. Using finite element analysis (FEA), Park et al. (2004) investigated the effect of continuous lateral bracing on the top flange (e.g., provided by concrete slabs) on the LTB resistance of wide flange beams. They compared their results against those based on standards equations and devised a moment gradient factor for the case where beams subjected to point loads.

Buckling solutions that account for web distortion include the work of Hancock et al. (1980) who developed an energy-based solution and Bradford and Trahair (1981) who developed a finite element solution for the distortional lateral torsional buckling analysis of beams. Bradford (1988) developed an approximate solution where lateral/torsional restraints are provided at the tension flange. Samanta and Kumar (2008) investigated the distortional buckling beams braced at the top flange, bottom flange or both flanges through shell FEA under Abaqus.

In the current study, three lateral torsional buckling solutions are provided for two case studies. The first solution is based on the beam finite element developed by Barsoum and Gallagher (1970) (Section 2.1). The second solution is based on a new distortional element (Section 2.2). The third solution (Section 2.3) is based on a shell FEA solution using Abaqus (SIMULIA 2012).The effect of lateral bracing at the top, bottom or both flanges on the critical moments is determined and comparisons are made. The effect of unbraced cantilever span on distortional buckling is investigated for cases where the load is applied at the shear center.

2 FINITE ELEMENT MODELS

This section describes the three types of finite element models adopted in the present study.

2.1 Barsoum and Gallagher element (BG)

The thin-walled beam finite element in (Barsoum and Gallagher (1970)) with two end nodes and three pre-buckling degrees of freedom and four buckling degrees of freedom per node (Figure 1). The nodal pre-buckling displacements are the longitudinal displacement, transverse displacement, and associated bending rotation while the nodal buckling displacements are the lateral displacement (for a doubly symmetric section the lateral displacement is defined at the shear center/centroid), the weak-axis rotation, the angle of twist and warping deformation. In Figure 1a, all displacements are shown with single red arrows, rotations are depicted with double-headed blue arrows while warping deformations is depicted by triple-headed green arrows. The element is originally formulated to model lateral restraints at the section shear center (by restraining the displacement v at the relevant nodes) and/or twist at a section (by restraining the angle of twist θ_x). Given that the present study aims at investigating the effect of lateral bracing at top or bottom flanges, the Barsoum and Gallagher element has been modified in the present study to incorporate kinematic constraints of the type $v \pm (h/2)\theta_x = 0$, where h is the section height (Sahraei et al. (2016)).

2.2 Distortional element (D)

The distortional LTB finite element developed in (Pezeshky et al. (2016)) is adopted for the analysis. The element is a 1D beam element with two end nodes and 3 pre-buckling DOFs (in a manner similar to the BG element) and 8 buckling DOFs per node (Figure 1b). These are the lateral displacement v and angle of twist θ and their derivatives v' and θ' at each of the top and bottom flanges. As a convention, subscript 'T' denotes nodal displacements at the top flange and subscript 'B' denotes those at the bottom flange. In the formulation of the beam element, the flanges are treated as independent Vlasov beams to capture global warping effects. In addition, the kinematics of Gjelsvik (1981) were adopted to account for local warping effects. In contrast to Vlasov beam kinematics which postulate the web to move a rigid bar in the plane of

cross-section, the web is treated as a flexible plate that follows the thin-plate kinematics of the Kirchhoff plate bending theory (1850). As a simplification, the web lateral displacement is assumed to follow a cubic distribution across the web height (Figure 2). Besides capturing web distortion, the element is able to model top and/or bottom flange lateral and torsional restraints in a natural way by restraining the corresponding nodal lateral displacements u_T, u_B and/or angles of twist θ_T, θ_B when needed. The case of mid-height lateral bracing is not supported in the present version of the element.

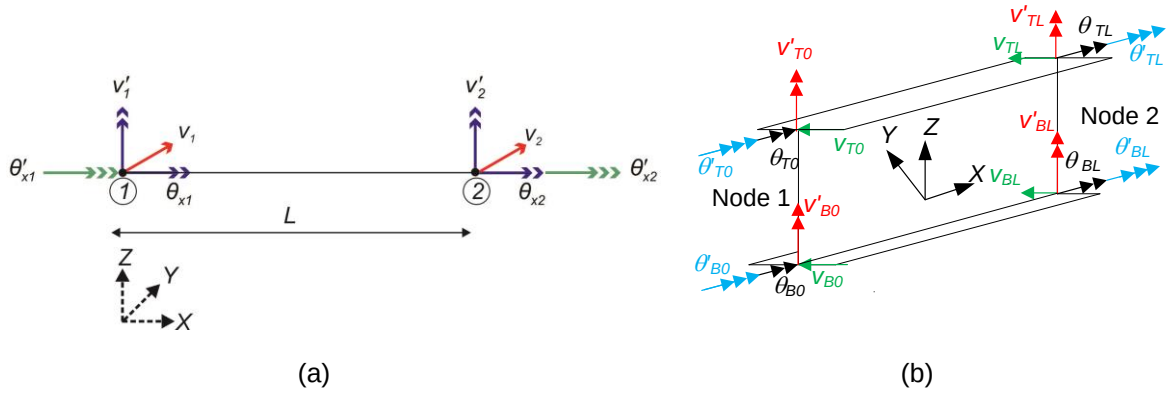

Figure 1: Buckling DOFs of a) Barsoum and Gallagher beam element b) distortional beam element

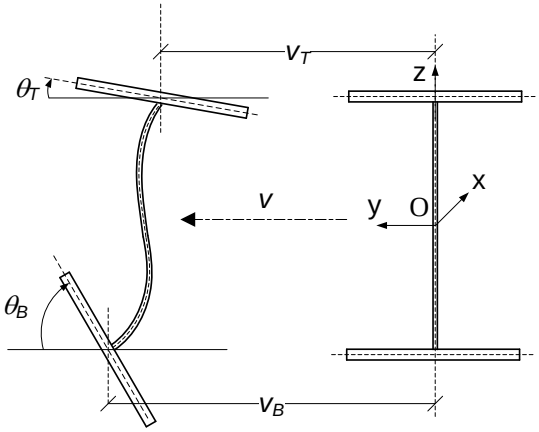

Figure 2 Displacement fields of web distortion

2.3 **S4R shell model**

The S4R shell element in the Abaqus library has been adopted to mesh the flanges and web of the beams. The S4R element is a 4-node quadrilateral element with 6 degrees of freedom per node and reduced integration. The beam is meshed typically using 240 elements along the length, 8 elements across the web height and 8 elements to model each of the flanges. For cases involving shear center loading, in order to suppress localized deformation that may arise in the model under point loads at web mid-height (that may not exist in practical situations where loads are applied over a finite area), the point load Q was divided into two contributions, each with a magnitude $Q/2$, and applied at the top and bottom of web to flange junctions. A linearized eigen-value buckling solution of the type

$$[1]\left(\left[K_E\right]+\lambda\left[K_G\right]\right)\{u\}=\{0\}$$

was sought under each the three models in Sections 2.1-2.3, where $[K_E]$ is the elastic stiffness matrix, $[K_G]$ is the geometric stiffness matrix, λ is the eigenvalue which characterizes the buckling load magnitude, and the eigen-mode $\{u\}$ is the associated buckling mode.

3 EXAMPLES

Three examples are presented to study and illustrate the effect of bracing type on LTB resistance of simply supported beams and cantilevers.

3.1 Example 1: Simply supported beam under point load

A simply supported beam with a W310x28 cross-section and span L = 6.00m, is subjected to a point load located at $0.6L$ as shown in Figure 3. The load is assumed to act at the shear center. End sections are assumed to be restrained from lateral restraint and twist. Five lateral bracing scenarios are considered at the section of loading: (top flange bracing, shear center bracing, bottom flange bracing, bracing at both flanges, and no bracing). It is required to determine the elastic lateral torsional buckling resistance of the beam in each case. The BG and distortional models are discretized into 8 elements and the results are summarized in Table 1.

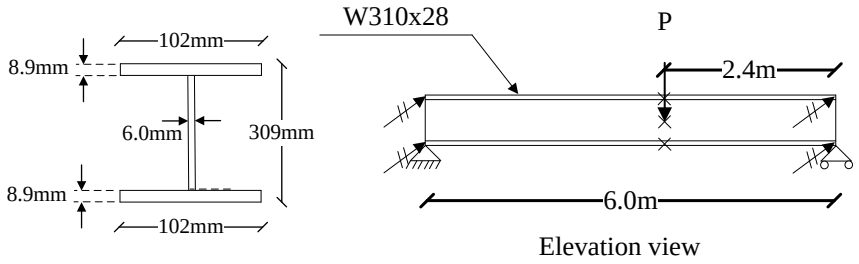

Figure 3: Simply supported beam under point load

Table 1: Comparison of buckling loads for various bracing scenarios at 0.6L

Brace Location	(1) Abaqus Shell FEA (kN)	(2) Distortional Element D (kN)	(3) BG Element (kN)	(4) =(3)/(1) =D/Abaqus	(5) =(4)/(1) =BG/Abaqus
Top Flange	78.2	81.2	86.4	1.04	1.10
Shear Center	78.5	-	87.1	-	1.11
Bottom Flange	26.3	27.1	30.0	1.03	1.14
Both Flanges	78.8	81.9	87.1	1.04	1.11
No Brace	22.3	23.1	24.8	1.04	1.11
Maximum	-	-	-	1.04	1.14
Minimum	-	-	-	1.03	1.10
Average	-	-	-	1.04	1.11

The critical load for the case of no bracing as predicted based on the critical moment equation in CAN/CSA-S16 (2014) is found 24.4kN. This value nearly coincides with that based on the BG solution since both solutions do not account for distortional effects. As expected, the S4R solution and the distortional element solutions provide slightly lower critical load predictions as both account for web distortion. For the case of both flange restraints, the critical load predicted by CAN/CSA-S16 (2014) is 61.7kN and ANSI/AISC-360 (2016) is 62.8kN. Both values compare to 87.1 kN as predicted by the BG elements. While all three solutions suppress distortion effects, the CAN/CSA-S16 (2014) and ANSI/AISC-360 (2016) do not account for the interaction between the left and right spans, whereby the right span, having a smaller span tends to delay

buckling of the left span having the longer span. This issue is addressed in more details in (Sahraei et al. (2016)). In contrast, the present BG solution is able to account for the interaction between both spans in a natural way.

Column (4) of Table 1 shows that the ratio of the critical loads as predicted by the distortional element to that based on the Abaqus S4R element ranges between 1.03 and 1.04 and averages 1.04. While both models account for web distortion, the 4% difference between the results of both models can be attributed to the fact that while the S4R model discretizes the web height into multiple segments, the distortional element is based on a cubic lateral displacement approximation, which provides a slightly stiffer representation of the web response, and thus results in a slightly higher predicted buckling loads. The modelling and computational effort for the distortional element is significantly lower than the shell model.

Column (5) shows that the ratio of the critical loads as predicted by the BG element to that based on the Abaqus shell FEA ranges between 1.10 and 1.14 and averages 1.11. The difference is attributed to (a) while the properties input into the BG model account for the presence of fillets, those based on the shell model omit fillet effects, and (b) the web distortional effects which are captured in the shell model but not in the BG elements. The predicted buckled configurations based on the shell FEA, the distortional element, and the BG element are provided in Figure 4 for all five problems solved. In all cases, the buckling modes were normalized with respect to the peak lateral displacement at the top flange. For each solution, the lateral displacement for of the top flange, the shear center, and the bottom flange are depicted respectively in black, red, and blue. The mode shapes based on all three models nearly coincide in all cases, except for the case of the shear center brace where the mode shapes show a similar trend with a small difference in the displacement magnitudes.

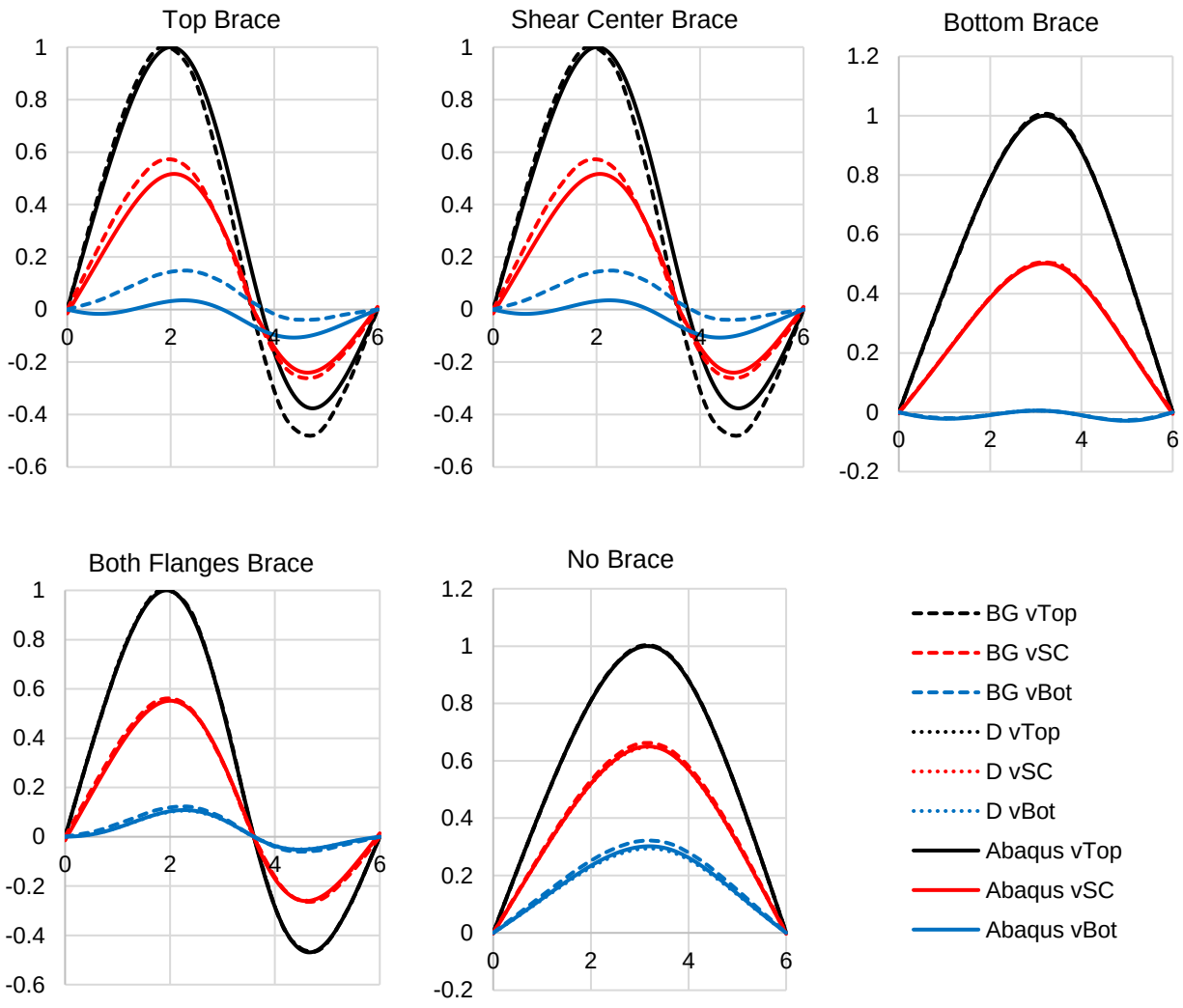

Figure 4: Comparison of buckling mode shapes

3.2 **Example 2: Long span cantilevers**

A cantilever has a 6.00m span and a W200x59 cross-section (cross-section dimensions are shown in Figure 5). The member is subjected to a load acting at the tip and located at the shear center. For a yield stress of $F_y = 350MPa$, section class is 1 and the corresponding plastic moment is 229 kNm. Five bracing scenarios are considered at the tip (top flange bracing, shear center bracing, bottom flange bracing, both flanges braced and no bracing). It is required to determine the lateral torsional buckling resistance for the five cases.

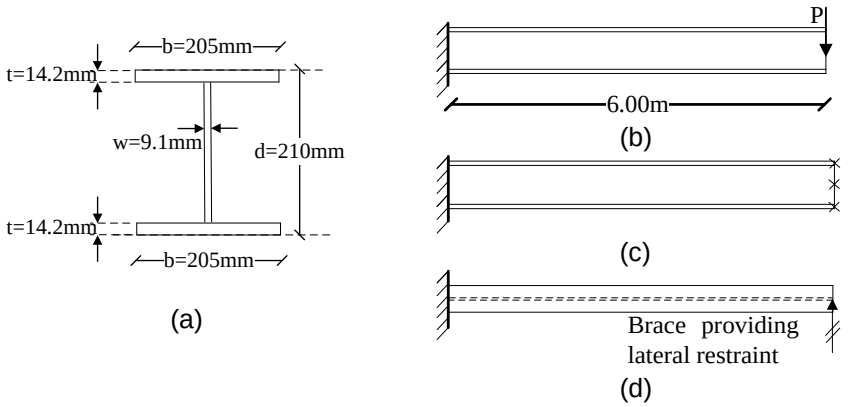

Figure 5: a) Cross section dimensions, b) 6.0m cantilever subjected to tip load, c) possible locations of lateral braces, d) plan view showing the lateral support

Meshes identical to Example 1 are used for each model. Column (4) of Table 2 shows that the ratios of the critical loads as predicted by the distortional element (D) to those based on the Abaqus S4R solutions range between1.02 to 1.04 and average 1.02. As discussed in example 1, since the lateral displacements in the D element are assumed to have a cubic distribution along the web height, the D model provides a slightly higher representation of the stiffness compared to the more flexible shell element. Column (5) shows that the ratio of the critical loads as predicted by the BG element to that based on the Abaqus S4R solution ranges between 1.05 and 1.08 and averages 1.06. Again, the difference is attributed to (a) presence of fillets which are captured by the properties input to the BG model but not into the shell model, and (b) distortional effects which are captured in the shell model but not in BG elements. The BG element provides the stiffest representation of all solutions since the lateral displacements of the web is assumed to vary linearly with the height as implied by the first Vlasov assumption. All three models suggest that the case of top flange bracing is more effective in increasing the buckling load than shear center bracing or bottom flange bracing. As expected, the case of no bracing corresponds to the lowest predicted load while the case of top and bottom bracing corresponds to the highest predicted critical load. For the case where both flanges are braced, the member tip becomes restrained against twist and lateral displacement, and the CAN/CSA-S16 (2014) moment can be adopted to provide a conservative prediction for the critical load. For such a case, the unsupported length is 6m and the moment gradient factor is 1.75, and the predicted critical load is 64.9kN which compares to 149.2kN based on the BG solution. The difference between both solutions is attributed to the fact that for the present problem the warping deformation and weak axis rotation at the cantilever root are restrained while the CAN/CSA-S16 (2014) equation is based on free warping and weak axis rotation. The buckled configurations based on the shell FEA, the distortional element, and BG are provided in Figure 6 for all five problems. In all cases, the mode shapes based on all three models are observed to nearly coincide.

Table 2: Comparison of buckling loads

Bracing location	(1) Abaqus Shell FEA (kN)	(2) Distortional Element D (kN)	(3) BG Element (kN)	(4)=(3)/(1) D/Abaqus	(5)=(4)/(1) BG/Abaqus
Top Flange	105	109	114	1.04	1.08
Shear Center	86.9	-	91.4	-	1.05
Bottom Flange	70.7	72.3	74.6	1.02	1.06
Both Flanges	140.3	140.8	149.2	1.00	1.06
No Brace	59.7	61.8	62.4	1.03	1.05
MAX.	-	-	-	1.04	1.08
MIN.	-	-	-	1.02	1.05
AVG.	-	-	-	1.02	1.06

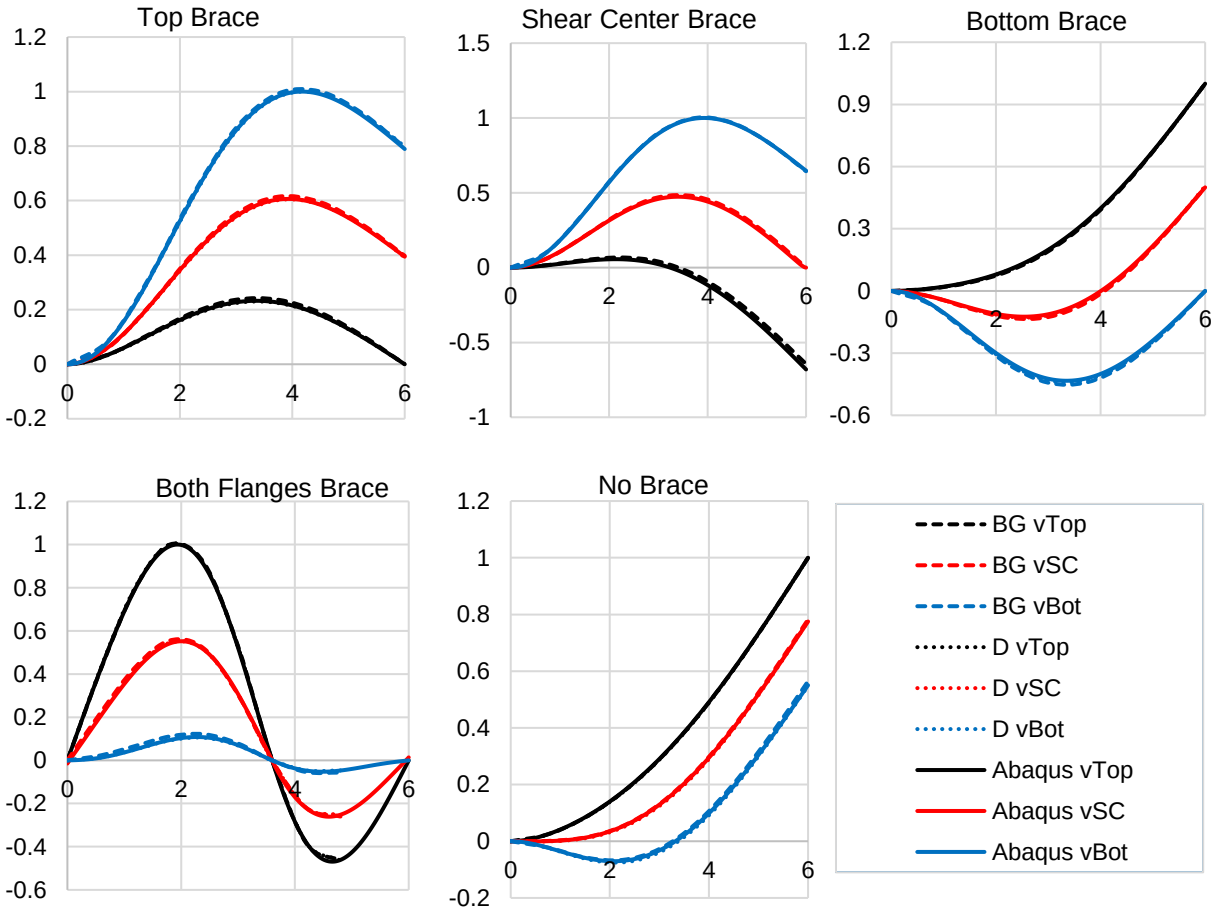

Figure 6: Comparison of buckling mode shapes

3.3 **Example 3: Effect of cantilever span**

Example 2 is revisited for the case of no bracing. Spans are varied from 2.00 to 6.00m in order to investigate the effect of span on distortion. Comparisons between the predictions of the BG and D are provided in Table 3. As seen, as the span decreases from 6.00 to 2.00m, the ratio of the critical loads based on the BG element to that based on the D element increases from 1% to 14%, indicating that the effect of distortion becomes more tangible in short span cantilevers. The results are depicted in the plot in Figure 7 and the mode shapes for various spans are depicted in Figure 8.

Table 3 Comparison of buckling loads

(1) Span (m)	(2) Buckling Load (kN) D	(3)Buckling Load (kN) BG	(4)=(3)/(2)
2	842	957	1.14
3	328	339	1.03
4	163	166	1.02
5	95.4	96.4	1.01
6	61.8	62.4	1.01

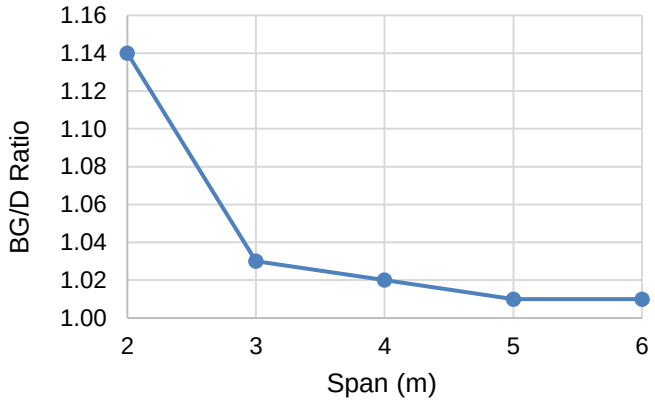

Figure 7: Ratio of critical moments versus span

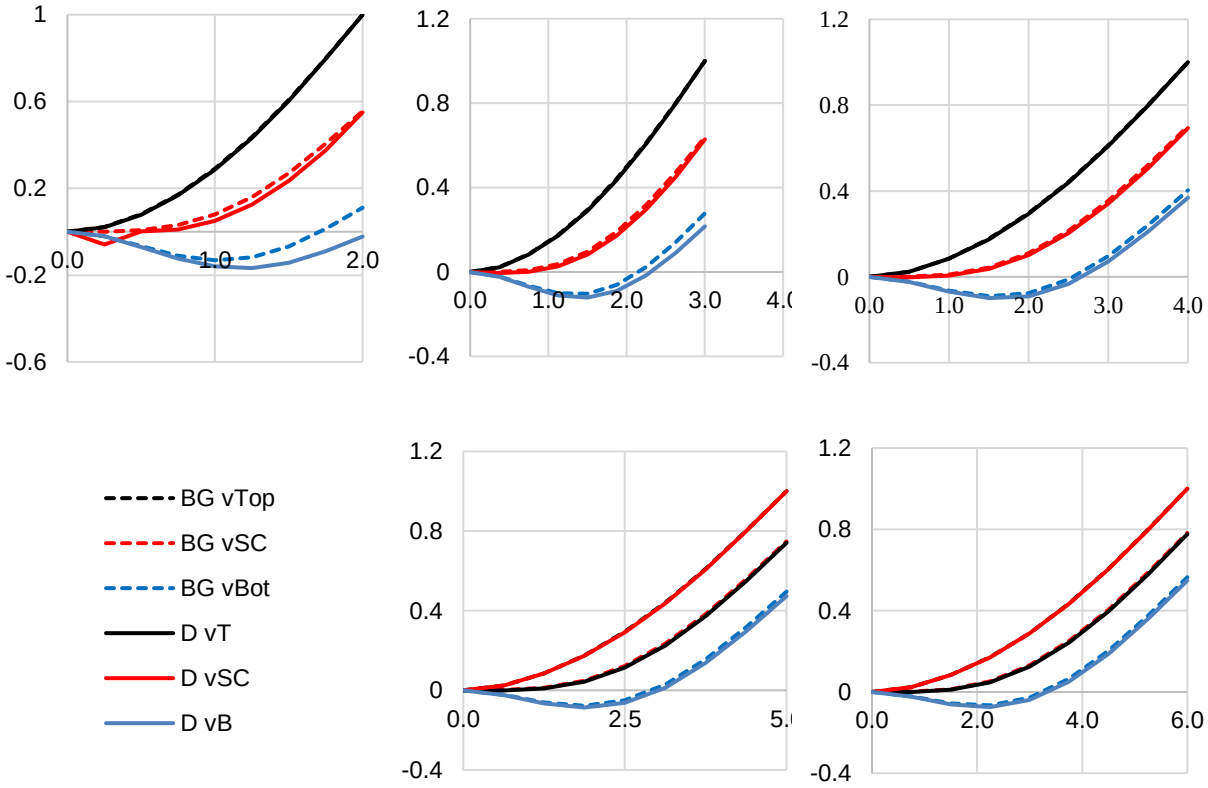

Figure 8: Buckling mode shapes for various spans of Example 3 (no bracing – shear center loading)

4 CONCLUSIONS

The following conclusions can be drawn: (1) The present study developed, implemented, and established the validity of two finite elements as part of a larger project aimed at integrating them within the commercial S-FRAME analysis software and S-STEEL structural steel design software. (2) For the simply supported beam under point load investigated, the buckling load predicted by all three models is highest when the brace is provided either at the shear center, at the top flange, or at both flanges. (3) For the same problem, bracing the bottom flange laterally results in a slight gain in the predicted buckling load compared to the case on no bracing. Moving the bracing either to the shear center or to the top flange corresponds to a significant increase in the predicted critical load. (4) For the cantilever problem investigated, the lateral

bracing scenarios sorted in descending order of effectiveness are: both flange bracing, top flange bracing, shear center bracing, bottom flange bracing, and no bracing. (5) Distortional effects are significant for short cantilevers and loose significance as cantilever spans increase. (6) The modified BG element provides results comparable to provisions of CAN/CSA-S16 (2014) as both supress distortional effects while the distortional element D provides results that are comparable to shell FEA as they both account for distortional effects.

5 Acknowledgements

The authors wish to express their gratitude of Mr. George Casoli, Dr. Feng Rong, Dr. Siriwut Sasibut, and Dr. Marinos Stylianou, from S-Frame Software Inc. for their instructive feedback and effort. Financial support from the S-Frame Software Inc. and matching funds from Natural Sciences and Engineering Research Council (NSERC) of Canada is also gratefully acknowledged.

6 REFERENCES

ANSI/AISC-360 (2016). "ANSI/AISC 360-16." *Specification for structural steel buildings*, American Institute of Steel Construction (AISC), Chicago, IL.

Barsoum, R. S., and Gallagher, R. H. (1970). "Finite element analysis of torsional and torsional–flexural stability problems." *International Journal for Numerical Methods in Engineering*, **2**(3), 335-352.

Bradford, M. A. (1988). "Buckling of elastically restrained beams with web distortions." *Thin-Walled Structures*, **6**(4), 287-304.

Bradford, M. A., and Trahair, N. S. (1981). "Distortional Buckling of I-Beams." *Journal of the Structural Division, ASCE*, **107**(2), 355-370.

CAN/CSA-S16 (2014). "Limit states design of steel structures." *Standard CAN/CSA-S16-14*, Canadian Standards Association, Mississauga, Ontario.

Gjelsvik, A. (1981). *The theory of thin walled bars / Atle Gjelsvik*, Wiley, New York, NY, USA.

Hancock, G. J., Bradford, M. A., and Trahair, N. S. (1980). "Web distortion and flexural-torsional buckling." *Journal of the Structural Division, ASCE*, **106**(7), 1557-1571.

Kirchhoff, G. (1850). "Ueber das Gleichgewicht und die Bewegung einer elastischen Scheibe." *crll*, **40**, 51-88.

Neville, J. R., Peter, F. D., and Sritawat, K. (1984). "Buckling and Bracing of Cantilevers."

Park, J. S., Stallings, J. M., and Kang, Y. J. (2004). "Lateral–torsional buckling of prismatic beams with continuous top-flange bracing." *Journal of Constructional Steel Research*, **60**(2), 147-160.

Pezeshky, P., Sahraei, A., and Mohareb, M. (2016). "Distortional lateral torsional buckling of wide flange steel beams." University of Ottawa, Internal report submitted to S-Frame Software INC.

Sahraei, A., Pezeshky, P., and Mohareb, M. (2016). "Lateral torsional buckling of wide flange steel beams - finite element formulation." University of Ottawa, Internal report submitted to S-Frame Software INC.

Samanta, A., and Kumar, A. (2008). "Distortional buckling in braced-cantilever I-beams." *Thin-Walled Structures*, **46**(6), 637-645.

SIMULIA. 2012. Abaqus/CAE Analysis, version 6.12-3, Dassault Systemes.

Trahair, N. S. (1993). *Flexural-torsional buckling of structures*, CRC Press, USA.

Vlasov, V. Z. (1961). *Thin walled elastic beams*, Israel Program for Scientific Translations, Jerusalem, Israel. Available from Office of Technical Services, US Department of Commerce,Washington, D.C.